Journal of Alloys and Compounds 404–406 (2005) 24–26

Journal of
ALLOYS
AND COMPOUNDS

www.elsevier.com/locate/jallcom

Study of the lithium–nitrogen–hydrogen system

G.P. Meisner[a,*], F.E. Pinkerton[a], M.S. Meyer[a],
M.P. Balogh[a], M.D. Kundrat[b]

[a] *GM Research & Development Center, Warren, MI 48090, USA*
[b] *Aerotek Corp., Warren, MI 48090, USA*

Received 28 May 2004; received in revised form 8 November 2004; accepted 12 November 2004

Abstract

We investigated lithium–nitrogen–hydrogen compounds as potential hydrogen storage materials and report consistent results for the amount of hydrogen gas sorbed, weight change, and phase content for our various samples. We observed a sluggish and incomplete reaction between hydrogen and lithium nitride of >7 wt.% hydrogen uptake at 160 °C with no observable hydrogen release into vacuum, and a ∼5.2 wt.% cyclable hydrogen sorption at 240 °C consistent with a reversible lithium amide/lithium imide reaction. The plateau pressure for the amide/imide reaction is quite low, ∼10 kPa at 240 °C.

Keywords: Hydrogen storage materials; Gas–solid reactions; X-ray diffraction

Using hydrogen-powered fuel cells for automotive transportation is an exciting conceptual solution for two major societal concerns: fossil fuel dependence and pollution. Implementation, however, requires technological breakthroughs, particularly regarding efficient production of large quantities of hydrogen from non-fossil fuel sources and practical on-board hydrogen storage. Considerable research is focused on new solid substances for hydrogen storage that include metal hydrides, physisorptive materials, and hydrogen compounds. So far it has not been possible to achieve all desirable material properties for hydrogen storage systems simultaneously in a single substance [1]. We report our research on new potential hydrogen storage materials in the lithium–nitrogen–hydrogen system [2–7].

We obtained lithium nitride (Li_3N) powder from Alfa Aesar, and our chemical analysis shows that it is 51 wt.% lithium (pure Li_3N is 59.8 wt.% lithium). Our X-ray diffraction (XRD) analysis reveals it to be a mixture of the room temperature form of Li_3N and the metastable high-pressure form (As_3Na-type), and that the major impurity phases are LiOH and Li_2O. We perform hydrogen (H_2) sorption experiments on as-received Li_3N powder using XRD, volumetric, and gravimetric techniques. For real-time in situ XRD experiments, we use Cu Kα radiation in a Bruker AXS General Area Detector Diffractometer System. We load and seal samples into 1 mm quartz capillary tubes and mount them in a sample cell and furnace, described previously [8], in an Ar gas glove box. We collect XRD data using an 0.8 mm collimator, 15 cm detector distance, goniometer angles of $\Omega = 20^\circ$ and $2\theta = 34^\circ$, and 1–5 min integration times. This allows collection of XRD data for angles $16^\circ < 2\theta < 51^\circ$. For isothermal volumetric experiments, we use a commercial Gas Reaction Controller, described previously [9,10], and measure equilibrium pressures and temperatures to accurately determine amounts of gas in the various chambers of the apparatus. For gravimetric experiments, we use a Cahn Model 2151 high-pressure thermogravimetric analyzer (TGA) [11,12]. Carefully weighed ∼300 mg powder samples are placed into quartz sample buckets and covered with pentane to protect them from exposure to air when removed from the glove box for loading into the TGA. The TGA is thoroughly purged with He gas while the pentane evaporates completely. Hydrogen sorption is directly measured as weight changes after correct-

---

[*] Corresponding author. Tel.: +1 586 986 0626; fax: +1 586 986 3091.
E-mail address: gregory.p.meisner@gm.com (G.P. Meisner).

0925-8388/$ – see front matter © 2005 Elsevier B.V. All rights reserved.
doi:10.1016/j.jallcom.2004.11.103

ing for non-gravitational forces on the electrobalance due to buoyancy, gas flow velocity, and electrobalance temperature.

We reacted Li_3N with H_2 according to the equations:

$$Li_3N + 2H_2 \rightarrow Li_2NH + LiH + H_2 \quad (1)$$

$$Li_2NH + LiH + H_2 \leftrightarrow LiNH_2 + 2LiH \quad (2)$$

These reactions are sufficiently exothermic that, with the excess H_2 typically present in our high-pressure experiments, they proceed to the right and ultimately toward the completion of Eq. (2). The resulting mixture of $LiNH_2$ and LiH in a 1:2 molar ratio is consistent with our in situ XRD, volumetric, and TGA experiments presented below. Chen et al. [2] have shown that full reversal to Li_3N requires high temperatures, hence the conditions of the reaction described by Eq. (2) are more compatible with practical reversible H_2 storage.

We performed in situ XRD measurements on Li_3N initially in 550 kPa H_2 and then heated to ∼160 °C. The temperature was then increased in 15 °C increments over 1800 min to 235 °C. At ∼1860 min, the H_2 was evacuated using a mechanical vacuum pump for ∼960 min. Finally, at ∼2850 min, the sample holder was pressurized to 625 kPa H_2. The in situ XRD data for Li_3N contain more than 1000 diffraction patterns collected during this ∼ 50 h experiment, and Fig. 1 shows representative patterns resulting from hydriding and de-hydriding Li_3N. The room temperature diffraction pattern shows a weak but detectible diffraction peak at $2\theta \approx 30.5^\circ$ that is not observed prior to the initial H_2 pressurization, and we attribute it to a reaction of H_2 with Li_3N forming $LiNH_2$ and/or lithium imide (Li_2NH). During hydriding, the diffraction pattern at 2 min and ∼160 °C shows increasing peak intensity for $LiNH_2$, and at 1800 min and 235 °C shows increasing peak intensity for $LiNH_2$ and LiH and decreasing peak intensity for Li_3N, consistent with Eqs. (1) and (2). During de-hydriding, the diffraction pattern at 2400 min and 253 °C shows a mixture of Li_2NH and LiH. Because $LiNH_2$ and Li_2NH have very similar diffraction patterns due to very similar crystal structures, the strongest diffraction peak for each phase has a nearly identical position at $2\theta \approx 30.5^\circ$, and consequently the intensity of this peak remains relatively constant during de-hydriding. We monitor the decomposition of $LiNH_2$ into Li_2NH according to the reverse of Eq. (2) by observing the disappearance of low intensity diffraction peaks unique to $LiNH_2$ (e.g., $2\theta \approx 17^\circ$ and 20° in Fig. 1) and the decrease in intensity of diffraction peaks from LiH. Finally, the Li_3N peaks we observe during de-hydriding are due to unreacted material remaining from the initial hydriding step.

Isothermal volumetric measurements of the hydriding and de-hydriding of Li_3N are shown in Fig. 2. The initial hydriding measurements of Li_3N typically show non-equilibrium effects and do not represent true equilibrium pressure-composition isotherms. Although the data acquisition program waits until the pressures and temperatures do not change significantly (i.e., until the H_2 gas is in equilibrium with the apparatus), that time interval is not long enough to ensure that the sample is in thermodynamic equilibrium with the H_2 gas at 1500 kPa and 159 °C. This is evident by the hydriding curve decreasing as the H_2 content increases (■ in Fig. 2) and reaching a minimum near 3 wt.%. We also observed the same non-equilibrium behavior in the initial hydriding curve of another sample measured at 164 °C (not shown). Hydriding is thus quite slow at these temperatures. We observe no de-hydriding into vacuum, however, implying that the kinetics of H_2 release is extremely slow. A second hydriding and de-hydriding cycle at 159 °C (Δ in Fig. 2) shows only small additional H_2 uptake and, again, no H_2 release. The total H_2 absorbed by Li_3N in this experiment is $(\text{mass } H_2)/(\text{mass } Li_3N + \text{mass } H_2) = 7.2$ wt.%. The total expected H_2 content from Eq. (1) is 5.47 wt.% and Eqs. (1) and (2) is 10.37 wt.% relative to the initial starting weight of the Li_3N sample. Thus, the hydriding reaction is not complete in the time allowed for the 159 °C experiment (first run: 83 h, second run: 25 h). The sample was then de-hydrided at 240 °C in dynamically pumped vacuum for ∼12 h. a third hydriding cycle (○ in Fig. 2) indicates that the amount of cyclable H_2 at 240 °C is 5.2 wt.% relative to the initial Li_3N sample weight. This result is smaller than the total H_2 absorbed previously,

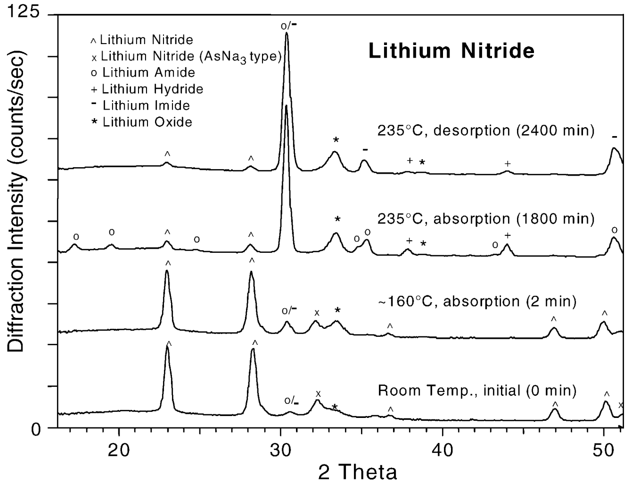

Fig. 1. Representative in situ X-ray diffraction data for hydriding and de-hydriding Li_3N.

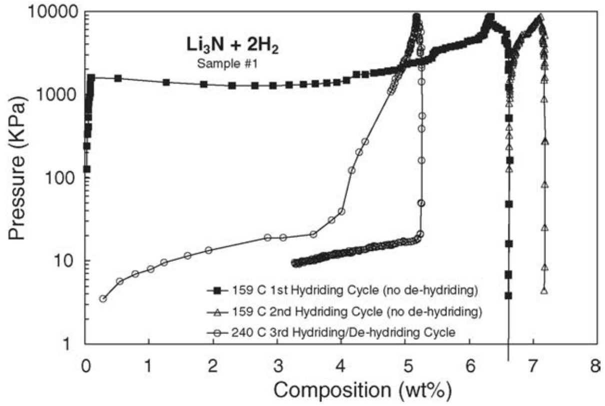

Fig. 2. Isothermal volumetric measurement of the hydriding and de-hydriding Li_3N plotted vs. log pressure.

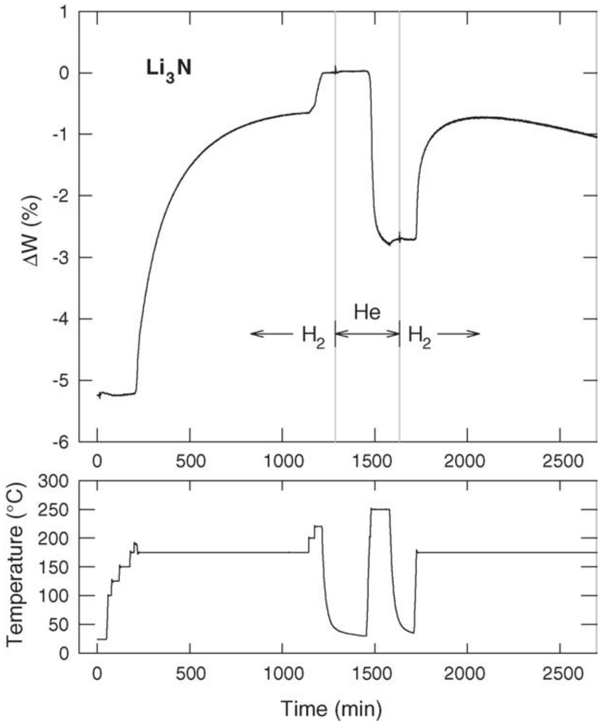

Fig. 3. Weight change with time during H_2 cycling of Li_3N. The lower panel shows the temperature profile.

but it is consistent with the reversible reaction described by Eq. (2), namely: (mass of cyclable H_2)/(mass Li_3N + mass of cyclable H_2) = 5.47 wt.%. The plateau pressures obtained are quite small, ∼10 kPa (see Fig. 2), so that de-hydriding is inhibited when only a small H_2 pressure develops in the sample chamber.

Gravimetric measurements of the hydriding and de-hydriding cycle of Li_3N are shown in Fig. 3, where ΔW is measured relative to the weight in the hydrided state. Starting from Li_3N in flowing H_2 at 136 kPa, H_2 absorption begins at ∼175 °C where the sorption kinetics are slow: ∼4.5 wt.% H_2 uptake in ∼1000 min. Further increasing the temperature boosts H_2 absorption to 5.2 wt.% at 220 °C. After cooling back to low temperature and changing the gas flow to He at 136 kPa, H_2 is released upon heating to 250 °C. The total quantity of H_2 released is 2.8 wt.%, or just over half of the original quantity absorbed. This is again consistent with the conclusion that the initial weight gain corresponds to the two-step reaction described by Eqs. (1) and (2), whereas de-hydriding under these conditions corresponds to only Eq. (2).

The sample re-hydrides after returning the gas flow to H_2 at 136 kPa and then heating to 175 °C. The weight reaches a peak after regaining about 2 wt.%, then decreases again and ultimately reaches an approximately constant rate of weight loss. This weight loss is due to production of ammonia (NH_3) (see, e.g., Ref. [3]). The peak near 2100 min (and presumably also near 1100 min) occurs when the rate of H_2 uptake equals the rate of NH_3 production. We emphasize that the rate of NH_3 production is very slow; the loss of ∼1 wt.% over ∼1000 min in H_2 represents the conversion of about 2% of the sample. We find that decomposition stops when the sample is below ∼150 °C, where decomposition by NH_3 release is kinetically excluded.

Acknowledgements

Thanks to G.G. Tibbetts, C.H. Olk, J.J. Vajo, J.J. Moleski, J.F. Herbst, S.J. Swarin, J.A. Spearot and M.W. Verbrugge.

References

[1] F.E. Pinkerton, B.G. Wicke, Ind. Phys. 10 (2004) 20.
[2] P. Chen, Z. Xiong, J. Luo, J. Lin, T.K. Tan, Nature 420 (2002) 302.
[3] Y. Hu, E. Ruckenstein, J. Phys. Chem. A 107 (2003) 9738.
[4] Y. Hu, E. Ruckenstein, Ind. Eng. Chem. Res. 42 (2003) 5135.
[5] T. Ichikawa, S. Isobe, N. Hanada, H. Fujii, J. Alloys Compd. 365 (2004) 271.
[6] T. Ichikawa, N. Hanada, S. Isobe, H. Leng, H. Fujii, J. Phys. Chem. B 108 (2004) 7887.
[7] Y. Nakamori, S. Orimo, J. Alloys Compd. 370 (2004) 271.
[8] M.P. Balogh, G.G. Tibbetts, F.E. Pinkerton, G.P. Meisner, C.H. Olk, J. Alloys Compd. 350 (2003) 136.
[9] G.G. Tibbetts, G.P. Meisner, C.H. Olk, Carbon 39 (2001) 2291.
[10] G.P. Meisner, G.G. Tibbetts, F.E. Pinkerton, C.H. Olk, M.P. Balogh, J. Alloys Compd. 337 (2002) 254.
[11] F.E. Pinkerton, B.G. Wicke, C.H. Olk, G.G. Tibbetts, G.P. Meisner, M.S. Meyer, J.F. Herbst, J. Phys. Chem. B 104 (2000) 9460.
[12] F.E. Pinkerton, M.S. Meyer, G.G. Tibbetts, R. Chahine, Proceedings of the 11th Canadian Hydrogen Conference, Victoria, BC, Canada, (2001) pp. 633–642.